

Coexistence of orbital and quantum critical magnetoresistance in $\text{FeSe}_{1-x}\text{S}_x$ S. Licciardello,¹ N. Maksimovic,² J. Ayres,^{1,3} J. Buhot,¹ M. Čulo,¹ B. Bryant,¹ S. Kasahara,⁴ Y. Matsuda,⁴ T. Shibauchi,⁵ V. Nagarajan,² J. G. Analytis,² and N. E. Hussey^{1,*}¹*High Field Magnet Laboratory (HFML-EMFL) and Institute for Molecules and Materials, Radboud University, Toernooiveld 7, 6525 ED Nijmegen, The Netherlands*²*Department of Physics, University of California and Materials Science Division, Lawrence Berkeley National Laboratory, Berkeley, California 94720, USA*³*H. H. Wills Physics Laboratory, University of Bristol, Tyndall Avenue, BS8 1TL, United Kingdom*⁴*Department of Physics, Kyoto University, Sakyo-ku, Kyoto 606-8502, Japan*⁵*Department of Advanced Materials Science, University of Tokyo, Kashiwa, Chiba 277-8561, Japan*

(Received 13 March 2019; revised manuscript received 2 July 2019; published 10 September 2019)

The recent discovery of a nonmagnetic nematic quantum critical point (QCP) in the iron chalcogenide family $\text{FeSe}_{1-x}\text{S}_x$ has raised the prospect of investigating, in isolation, the role of nematicity on the electronic properties of correlated metals. Here we report a detailed study of the normal state transverse magnetoresistance (MR) in $\text{FeSe}_{1-x}\text{S}_x$ for a series of S concentrations spanning the nematic QCP. For all temperatures and x values studied, the MR can be decomposed into two distinct components: one that varies quadratically in magnetic field strength $\mu_0 H$ and one that follows precisely the quadrature scaling form recently reported in metals at or close to a QCP and characterized by a H -linear MR over an extended field range. The two components evolve systematically with both temperature and S substitution in a manner that is determined by their proximity to the nematic QCP. This study thus reveals the coexistence of two independent charge sectors in a quantum critical system. Moreover, the quantum critical component of the MR is found to be less sensitive to disorder than the quadratic (orbital) MR, suggesting that detection of the latter in previous MR studies of metals near a QCP may have been obscured.

DOI: [10.1103/PhysRevResearch.1.023011](https://doi.org/10.1103/PhysRevResearch.1.023011)

I. INTRODUCTION

Many strongly interacting electron systems lie in close proximity to a quantum critical point (QCP), realized by suppressing a finite temperature ordering transition to zero temperature via some nonthermal tuning parameter [1]. Metallic quantum critical systems exhibit anomalous transport and thermodynamic properties, including (but not restricted to) a T -linear resistivity at low temperatures [2–4] and a logarithmic divergence of the electronic specific heat [5]. Recently, a new feature of metallic quantum criticality was discovered in the transverse magnetoresistance (whereby the magnetic field is applied perpendicular to the current) in the iron pnictide compound $\text{BaFe}_2(\text{As}_{1-x}\text{P}_x)_2$ (Ba122) near its antiferromagnetic QCP [6]. In particular, the magnetoresistivity, when expressed as $\Delta\rho/T$ (where $\Delta\rho = \rho[H, T] - \rho[0, 0]$) was found to exhibit an unusual quadrature scaling form $\sqrt{1 + \gamma(\mu_B\mu_0 H/k_B T)^2}$ where $0.5 \leq \gamma \leq 1$ is a dimensional parameter, k_B is Boltzmann's constant, and μ_B is the Bohr magneton [6,7]. Thus, in addition to a T -linear resistivity at zero field, $\Delta\rho$ is found to vary linearly with magnetic field strength over a wide field range. A similar scaling of the

transverse MR was also reported recently in the electron-doped cuprate $\text{La}_{2-x}\text{Ce}_x\text{CuO}_4$ (LCCO), again near its antiferromagnetic QCP [8].

In ordinary metals, the low-field orbital MR $\delta\rho/\rho[0, T] = (\rho[H, T] - \rho[0, T])/\rho[0, T] \propto (\omega_c\tau)^2$ where $\omega_c = e\mu_0 H/m^*$ is the cyclotron frequency, m^* is the effective mass of the charge carriers, e is the electric charge, and τ the scattering time [9]. In the limit where $\omega_c\tau < 1$, $\delta\rho/\rho[0, T]$ thus varies quadratically with field and given that $\rho[0, T] \propto 1/\tau$, the transverse MR has a strong temperature dependence that often obeys another form of scaling, known as Kohler's scaling, in which plots of $\delta\rho/\rho[0, T]$ versus $(H/\rho[0, T])^2$ at different temperatures collapse onto a single curve [10]. In certain correlated metals, such as the hole-doped cuprates [11] and the heavy fermion CeCoIn_5 [12], a modified Kohler's scaling is observed, whereby plots of $\delta\rho/\rho[0, T]$ versus $(H/\tan\Theta_H)^2$ collapse onto a single curve, where $\tan\Theta_H$ is the tangent of the Hall angle. By contrast, the MR curves in Ba122 and LCCO display no intrinsic temperature dependence—they simply present a set of parallel curves (at high field) offset by the change in $\rho[0, T]$ [6–8,13].

At present, there is no consensus as to the origin of the quadrature form for the transverse MR in quantum critical (QC) metals nor for the violation of Kohler scaling in other highly correlated metals. Moreover, it is not known how these very distinct MR responses are related, if at all. In particular, there is, as yet, no system in which signatures of the different MR behavior have been shown to coexist, suggesting that they

*nigel.hussey@ru.nl

are forms associated with different limits (e.g., the low- and high-field limits or the behavior of systems located near or far from a QCP).

In this contribution, we report the observation of two additive components in the transverse MR of a series of $\text{FeSe}_{1-x}\text{S}_x$ single crystals that collectively span a QCP—in this case a nematic QCP. One component has a quadratic-in-field MR response up to the highest fields studied (in all S-doped samples), suggesting that this H^2 MR is not the limiting low-field form of the quadrature component, but something distinct, presumably reflecting the (near-)perfect compensation of the electron and hole carriers in this family of semimetals. The second component, obtained by subtracting the H^2 term, exhibits the quadrature scaling form to a very high degree of precision, unambiguously demonstrating its coexistence with the conventional, orbital contribution. By studying the evolution of the MR over such a wide range of dopings and temperatures, we are able to rule out the second component originating from Dirac cone states, as reported, for example, in the iron pnictides [14–16]. Rather, the two components are found to evolve systematically with both temperature and S substitution in a manner that is determined by the proximity to the QCP. This study thus reveals the coexistence of two charge sectors in a quantum critical system. Finally, comparison of the MR response of two samples with very different residual resistivities reveals a marked difference in the sensitivity of the two components to disorder.

II. NEMATIC QUANTUM CRITICALITY IN THE IRON CHALCOGENIDES

The iron chalcogenide family $\text{FeSe}_{1-x}\text{S}_x$ [crystal structure displayed in Fig. 2(a)] represents a class of quantum critical metals in which the QCP is due to electronic nematicity rather than antiferromagnetism [17–20]. Recently, the evolution of the (in-plane) resistivity across the nematic QCP was studied in high magnetic fields applied in the longitudinal field configuration ($\mathbf{H} // I // ab$) in order to suppress superconductivity while at the same time, minimizing the normal state MR [21]. To orientate the subsequent analysis and discussion, we reproduce in Fig. 1 a schematic of the low-temperature phase diagram of $\text{FeSe}_{1-x}\text{S}_x$ as deduced from the temperature-dependent exponent α of the in-plane resistivity across the doping series at temperatures below 30 K [21]. The top color scale in Fig. 1 denotes the magnitude of α at different T and x . At $x = x_c = 0.16$, $\rho[T]$ is T linear down to 1.5 K while on either side of the QCP, $\rho[T]$ is found to cross over to a T^2 dependence characteristic of a correlated Fermi liquid. A^* —the coefficient of the T^2 resistivity (once corrected for the growth in total carrier density with S doping)—was found to become strongly enhanced on approach to x_c (from either side), as indicated by the lower color scale. All these observations are consistent with those found in other quantum critical metals and suggest a strong coupling of the charge carriers to quantum fluctuations of the relevant order parameter.

It should be acknowledged here that there is currently no recognized theory for a T -linear resistivity down to $T = 0$ at a nematic QCP in a clean system [22]. While FeSe exhibits only nematic order below T_s , a spin-density-wave (SDW) state is found to be stabilized under applied pressure [23].

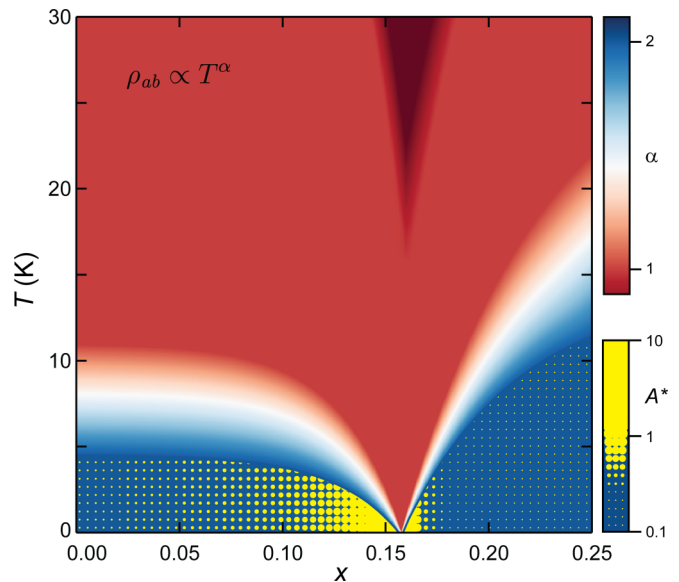


FIG. 1. Low-temperature phase diagram of $\text{FeSe}_{1-x}\text{S}_x$ described in terms of the exponent of the T -dependent resistivity that is itself defined in the upper color scale. The size of dots inside the T^2 regime indicate the strength of A^* , the coefficient of the T^2 resistivity, normalized to a fixed carrier density (and quantified in the lower color scale in units of $\mu\Omega \text{ cm K}^{-2}$) [21].

Moreover, enhanced spin fluctuations (at ambient pressure) and critical behavior have been reported below T_s [24,25], in the same range over which $\rho_{ab}[T]$ is quasi- T -linear, suggesting a possible link between the T -linear resistivity and antiferromagnetic, rather than nematic fluctuations. With increasing S substitution, however, the nematic and SDW states become decoupled [26], and as the pressure range of nematic order shrinks, eventually vanishing at x_c , the dome of SDW order shifts to progressively higher pressures. Thus, at $x = x_c$, the SDW phase is located far from the ambient pressure axis at which our experiments are performed. At the same time, NMR experiments have shown that spin fluctuations, although present in $\text{FeSe}_{1-x}\text{S}_x$ at low x values, are strongly suppressed with S substitution [27]. These combined results suggest that the critical behavior at $x = x_c$ is not associated with proximity to a magnetic phase.

III. METHODS

The single crystals of $\text{FeSe}_{1-x}\text{S}_x$ used in this study were grown at two different locations. The bulk of the samples were grown in Kyoto by the chemical vapor transport technique [17]. The actual sulfur composition x was determined by energy dispersive x-ray (EDX) spectroscopy, and was found to be around 80% of the nominal S content. The Berkeley sample discussed exclusively in Sec. V was grown using the KCl flux technique [28] with a nominal concentration of 18% selenium replaced by sulfur, whose composition was also confirmed by EDX. To be consistent with the data presented in Ref. [21] (carried out on the same Kyoto crystals), all x values quoted here are the nominal values. The crystals were cut into regularly shaped platelets and electrical contacts applied to each sample in a Hall bar geometry. The magnetotransport

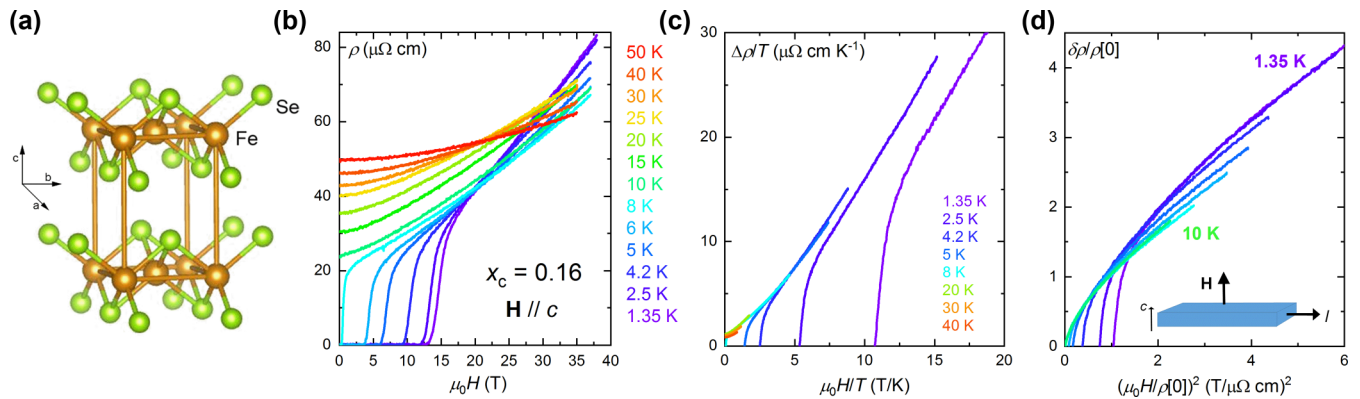


FIG. 2. (a) Crystal structure of FeSe. The brown (green) circles represent the iron (selenium) atoms. (b) Set of transverse MR curves for $\text{FeSe}_{0.84}\text{S}_{0.16}$ (i.e., at $x = x_c$) up to 38 T for $1.35 \text{ K} \leq T \leq 50 \text{ K}$ (individual T labels are given in the panels). Note the numerous crossing points—behavior distinct from that found recently in other QC systems [6–8]. (c) Test for QC scaling in $\text{FeSe}_{0.84}\text{S}_{0.16}$. Plot of $\Delta\rho/T$ versus μ_0H/T over the same temperature range, where $\Delta\rho/T = \rho[H, T] - \rho[0, 0]$. (d) Test for Kohler's scaling in $\text{FeSe}_{0.84}\text{S}_{0.16}$. Plot of $\delta\rho/\rho[0]$ versus $(\mu_0H/\rho[0])^2$ where $\delta\rho = \rho[H, T] - \rho[0, 0]$ and $\rho[0] = \rho[0, T]$. Inset: schematic showing the configuration of current and magnetic field used in this study.

measurements were carried out at the High Field Magnet Laboratory (HFML) in Nijmegen in a resistive Bitter magnet with a maximum field of 38 T using a combination of He-4 and He-3 cryostats and at the National High Magnetic Field Laboratory (NHMFL) in Los Alamos in a pulsed magnet with a field strength of 60 T. For the HFML experiments, the orientation of the samples with respect to the applied magnetic field was determined first using a Hall probe to orient the rotating platform, then the MR of the sample itself in order to locate the transverse field orientation more precisely.

IV. RESULTS AND ANALYSIS

A. Transverse magnetoresistance

Figure 2(b) shows a series of transverse MR ($H//c$) curves between 1.35 and 50 K for a $\text{FeSe}_{1-x}\text{S}_x$ single crystal with $x = x_c = 0.16$ whose in-plane resistivity was found to be T linear down to the lowest temperatures studied. In contrast to other quantum critical systems (i.e., Ba122 and LCCO), where the MR curves taken at different temperatures are found to be simply shifted vertically with respect to one another, $\delta\rho[\mu_0H]$ in $\text{FeSe}_{0.84}\text{S}_{0.16}$ is found to show a strong T dependence with multiple crossings. Consequently, when plotted as $\Delta\rho/T$ versus μ_0H/T [Fig. 2(c)] the MR sweeps do not fall onto a single curve, except in a narrow temperature range $4.2 \text{ K} \leq T \leq 20 \text{ K}$. Even in this intermediate range, however, the form of the MR does not follow the quadrature scaling ansatz. Moreover, as shown in Fig. 2(d), Kohler's scaling is not observed either. The same is true for the entire series of Kyoto samples that have been investigated.

The reason for this lack of scaling in either $\delta\rho/\rho[0, T]$ or $\Delta\rho/T$ becomes apparent when one inspects the derivative $d\rho/d(\mu_0H)$ of the individual MR curves. Panels (a) and (c) in Fig. 3 show $d\rho/d(\mu_0H)$ curves for $x = 0.10, 0.16$, and 0.25 , respectively, obtained at $T = 15 \text{ K}$, i.e., at a temperature where superconducting fluctuations are effectively suppressed. While the specific form of the derivative is most evident in the $x = 0.10$ sample [Fig. 3(a)], qualitatively similar behavior is found for all the other samples.

At the lowest fields, $d\rho/d(\mu_0H)$ is linear in the field with a zero intercept, implying that the low-field MR is strictly quadratic. The slope of the derivative is labeled $2\beta_0\mu_0H$ and is indicated in each case by a green dotted line. For $2\text{ T} < \mu_0H < 7 \text{ T}$, the slope of $d\rho/d(\mu_0H)$ gradually decreases until above 7 T, it becomes linear once more, albeit with a finite intercept. The presence of this finite intercept implies that for $\mu_0H > 7 \text{ T}$, the MR has two components, one linear in field, the other quadratic. A similar field-dependent MR was reported by Sun *et al.* for $x = 0$ and $x = 0.14$ albeit over a more limited field and temperature range [29]. In our study, both components are found to persist up to the highest field measured (35 T). Note that such a field dependence cannot be captured by a simple two-carrier model involving electrons and holes [30]. A three-carrier model [31] can produce an MR with a field dependence that resembles those displayed in Fig. 3, but only over a narrow range of field values and parameters. We will return to this point in the following section.

The slope of $d\rho/d(\mu_0H)$ at high field is defined here as $2\beta_{\text{FL}}$ where β_{FL} is the magnitude of the H^2 term that we argue below arises from orbital (i.e., cyclotron) effects. Upon subtracting this term from the total MR, the form of the second component in $\delta\rho[\mu_0H]$ is revealed. As indicated by the dotted black lines in panels (d) and (f), the remaining contribution to the MR is found to follow the same quadrature form, i.e., $\rho[\mu_0H] - \beta_{\text{FL}}(\mu_0H)^2 = a\sqrt{1 + b(\mu_0H)^2}$ that was first reported in $\text{BaFe}_2(\text{As}_{1-x}\text{P}_x)_2$ [6] (here a and b are fitting parameters). The quality of the fit, over the entire field range studied, appears to confirm that the transverse MR of $\text{FeSe}_{0.9}\text{S}_{0.1}$ comprises two distinct terms: one that is quadratic at all fields, and one that possesses the quadrature form (note that β_0 is a compound term, comprising both β_{FL} and the low-field quadratic part of the quadrature MR).

Further derivatives and residual MR curves for different samples recorded at different temperatures are presented in Fig. S1 of the Supplemental Material [32]. Significantly, the same features are observed for all x and T , albeit with different relative weightings, implying that these two distinct

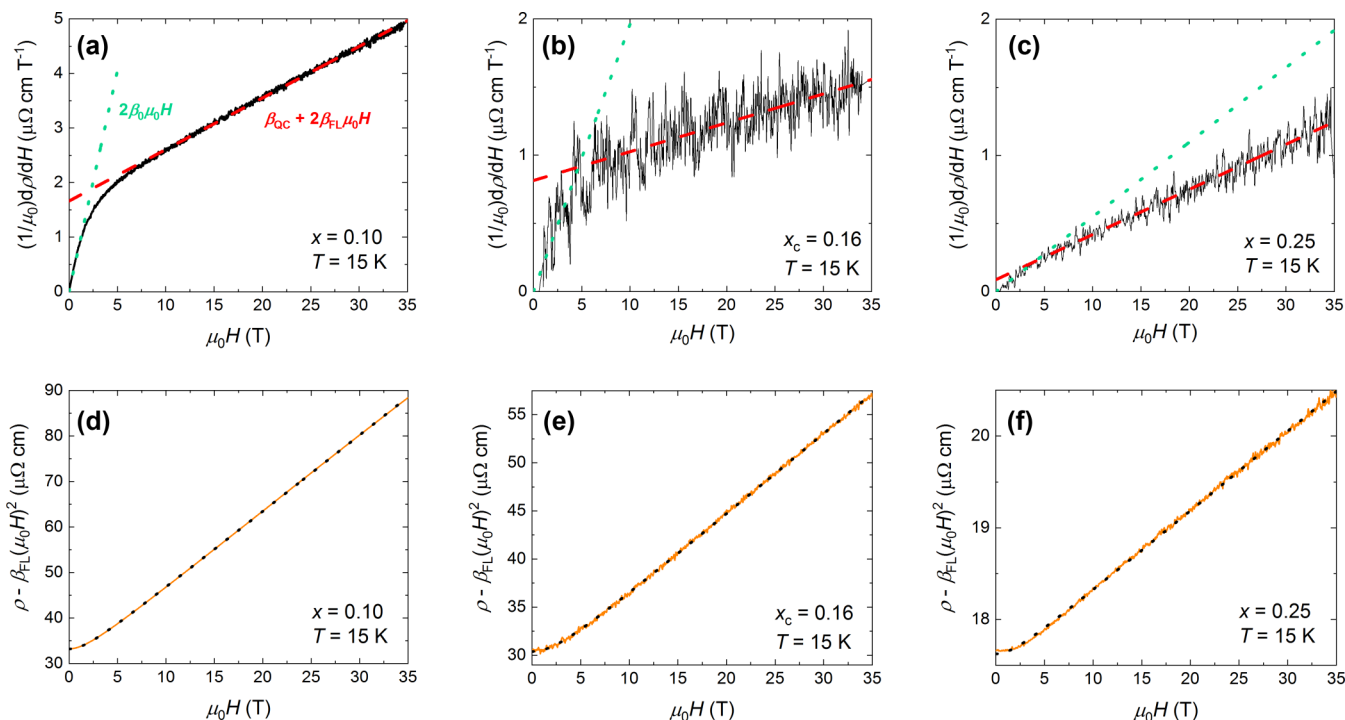


FIG. 3. $d\rho/d(\mu_0H)$ versus μ_0H at $T = 15$ K for (a) $x = 0.10$, (b) $x_c = 0.16$, and (c) $x = 0.25$. The dotted lines indicate the low-field H^2 dependence while the dashed lines highlight the high-field $H + H^2$ dependence. The magnitude of each component is labeled β_0 , β_{QC} , and β_{FL} as defined in the text. Upon subtraction of the high-field H^2 component, one obtains the corresponding “residual” MR terms shown in panels (d)–(f) for $x = 0.10, 0.16$, and 0.25 , respectively. The dotted lines are fits to the quadrature form $a\sqrt{1 + b(\mu_0H)^2}$.

MR contributions persist over the entire range of temperatures and S concentrations studied. Only in stoichiometric FeSe, where the orbital MR is extremely large, is this term found to deviate from H^2 at high fields and low T , though even here, the form of the MR (having subtracted off the quadrature component) is found to be consistent with the usual Drude expression for two-carrier (i.e., electron and hole) magnetotransport (see Fig. S2 in the Supplemental Material [32] for more details).

B. Two-component magnetoresistance

The data presented in Fig. 3 thus reveal the presence of two contributions to the MR response of $\text{FeSe}_{1-x}\text{S}_x$ which individually extend over a wide field, temperature, and doping range. A similar form of the MR has also been observed in the iron pnictide family $\text{Ba}(\text{Fe}_{1-x}\text{T}_x)_2\text{As}_2$ ($T = \text{Co, Ni, and Cu}$) [14–16]. There, as in $\text{FeSe}_{1-x}\text{S}_x$ [29], the H -linear component was attributed [14,15] to the MR response of Dirac-like states beyond the quantum limit [33]. A few reports have claimed evidence for the presence of Dirac cones inside the nematic phase of $\text{FeSe}_{1-x}\text{S}_x$ [29,34,35]. The fact that the H -linear MR component in $\text{FeSe}_{1-x}\text{S}_x$ persists beyond the nematic phase, however, suggests that it is unlikely that such Dirac-like states are responsible for the anomalous MR component found in $\text{FeSe}_{1-x}\text{S}_x$. There is also no reason *a priori* why the MR response of Dirac states should exhibit both the quadrature form and H/T scaling found in $\text{FeSe}_{1-x}\text{S}_x$ across the entire phase diagram (discussed in more detail in the following section).

The $H + H^2$ form of the MR in BaFe_2As_2 has also been modeled using a three-carrier Drude model [16]. While the three-carrier model is able to generate a MR curve that approximates a $H + H^2$ form (over a limited field range at least), it can only do so for a limited range of parameters. Moreover, for the same set of parameters, the corresponding Hall response is found to be highly nonlinear, whereas for $x \geq x_c$, the Hall resistivity of our crystals is found to be either linear or show only small deviations from linearity [36]. Finally, it is not possible to simulate the very different ratios of the H and H^2 terms observed in $\text{FeSe}_{1-x}\text{S}_x$ and over such a wide field range. Therefore, we do not believe it is appropriate to model the MR response in $\text{FeSe}_{1-x}\text{S}_x$ using the three-carrier model, at least one in which the carrier densities and mobilities are assumed to be independent of field strength. Of course, one could always add further complexity in the model (e.g., by allowing parameters to vary with field strength or introduce k dependence in a Boltzmann-type analysis), but in our opinion, this would not constitute a robust analysis.

The remarkable agreement between the “residual” MR (upon subtraction of the H^2 component) and the quadrature form of the MR, including the H/T scaling, leads us to conclude that the charge dynamics of $\text{FeSe}_{1-x}\text{S}_x$ must contain two distinct sectors: one that generates a conventional orbital MR, presumably involving quasiparticle transport, and one akin to the quantum critical sector found in Ba122 and LCCO (that exhibits scale invariance). In such a scenario, the total (zero-field) conductivity σ_{tot} should be expressed as a sum of the individual contributions, i.e., $\sigma_{\text{tot}}[T] = \sigma_{\text{QC}}[T] + \sigma_{\text{FL}}[T]$, where the subscripts refer to the quantum critical and

quasiparticle (Fermi-liquid) sectors, respectively. The transverse magnetoconductance is then given by a weighted sum [37]:

$$\frac{\Delta\sigma_{\text{tot}}}{\sigma_{\text{tot}}} = \frac{\sigma_{\text{QC}}}{\sigma_{\text{tot}}} \frac{\Delta\sigma_{\text{QC}}}{\sigma_{\text{QC}}} + \frac{\sigma_{\text{FL}}}{\sigma_{\text{tot}}} \frac{\Delta\sigma_{\text{FL}}}{\sigma_{\text{FL}}}. \quad (1)$$

In reality, of course, it is the magnetoresistance, rather than the magnetoconductance that is measured, the former being related to the latter via inversion of the (in-plane) conductivity tensor.

$$\frac{\delta\rho}{\rho[0, T]} = -\frac{\Delta\sigma_{\text{tot}}}{\sigma_{\text{tot}}} - \left(\frac{\sigma_{xy}}{\sigma_{\text{tot}}}\right)^2 \quad (2)$$

where $\rho[0, T] = 1/\sigma_{\text{tot}}$ is the zero-field resistivity at the temperature at which an individual field sweep is taken, σ_{xy} is the Hall conductivity, and $\sigma_{xy}/\sigma_{\text{tot}}$ the corresponding Hall angle. In order to proceed, it is necessary to estimate first the magnitude of the Hall angle ($\sigma_{xy}/\sigma_{\text{tot}}$) relative to $\delta\rho/\rho[0, T]$ (as measured). In the temperature range $20\text{K} < T < 50\text{K}$ over which we currently have data overlap, the square of the Hall angle (for $x = 0.16$) varies between 5% and 20% of the as-measured MR [36]. Thus, we can conclude that the MR is dominated by the magnetoconductance term and rewrite Eq. (1) as

$$\frac{\delta\rho}{\rho[0, T]} = \frac{\sigma_{\text{QC}}}{\sigma_{\text{tot}}} \frac{\delta\rho_{\text{QC}}}{\rho_{\text{QC}}[0, T]} + \frac{\sigma_{\text{FL}}}{\sigma_{\text{tot}}} \frac{\delta\rho_{\text{FL}}}{\rho_{\text{FL}}[0, T]}. \quad (3)$$

Hence,

$$\delta\rho[H] = \left(\frac{\sigma_{\text{QC}}}{\sigma_{\text{tot}}}\right)^2 \delta\rho_{\text{QC}}[H] + \left(\frac{\sigma_{\text{FL}}}{\sigma_{\text{tot}}}\right)^2 \delta\rho_{\text{FL}}[H] \quad (4)$$

which at high fields can be expressed as

$$\delta\rho[H] = \beta_{\text{QC}}\mu_0 H + \beta_{\text{FL}}(\mu_0 H)^2. \quad (5)$$

Here β_{QC} and β_{FL} are, respectively, the (as-measured) magnitudes of the H -linear and H^2 MR terms, which according to Eqs. (4) and (5) represent the quantum critical $\delta\rho_{\text{QC}}[H]$ and quasiparticle $\delta\rho_{\text{FL}}[H]$ contributions to the total MR, weighted by the square of the contribution of the two sectors to the total (zero-field) conductivity.

C. Evolution across the phase diagram

The ratio $\beta_{\text{QC}}/\beta_{\text{FL}}$ for all samples, determined at a temperature (15 K) at which there are no discernible superconducting fluctuation conductivities, is plotted in Fig. 4 (as open red circles). The ratio is found to peak around $x_c = 0.16$, in a manner that is strikingly similar to the enhancement of the quasiparticle effective mass as expressed through A^* , the renormalized coefficient of the T^2 resistivity (and plotted as empty black squares in Fig. 4) [21]. It is important to realize that these two quantities are determined in very different ways yet together, they appear to reveal a consistent picture in which the (magneto)transport properties of $\text{FeSe}_{1-x}\text{S}_x$ are heavily influenced by the presence of quantum critical fluctuations.

As described above, plots of $\Delta\rho/T$ versus H/T in P -doped Ba122 at the critical doping collapse onto a single curve of the quadrature form [6]. Such scaling can only be realized if the high-field (H -linear) slopes of the individual MR curves are the same, i.e., $\Delta\rho_{\text{QC}} = X_1\mu_0 H$ independent

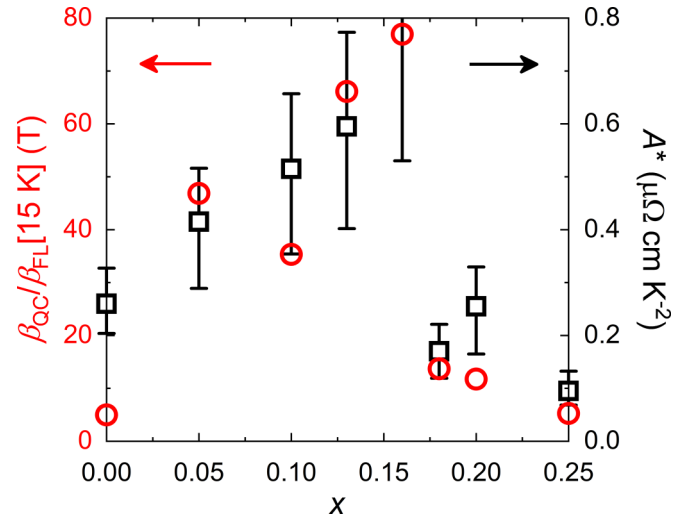


FIG. 4. Open circles: Variation of $\beta_{\text{QC}}/\beta_{\text{FL}}$, the ratio of the H -linear transverse MR to the (high-field) H^2 component as a function of x . All $\beta_{\text{QC}}/\beta_{\text{FL}}$ values were obtained at $T = 15\text{K}$. Open squares: Corresponding values of A^* , the coefficient of the T^2 resistivity, normalized to a fixed carrier density [21].

of temperature. Since there are two contributions to the MR in $\text{FeSe}_{1-x}\text{S}_x$, whose relative strengths are weighted by their respective contributions to the total conductivity, the same $\Delta\rho/T$ scaling cannot be gleaned directly from our data by simply subtracting off the orbital MR term. Nevertheless, further analysis outlined below and presented in Secs. III and IV of the Supplemental Material [32] provides strong evidence that H/T scaling is also realized in $\text{FeSe}_{1-x}\text{S}_x$.

Firstly, according to the scaling ansatz of Hayes *et al.* [6], the residual MR (obtained by subtracting the H^2 term from the total MR) should have the same dependence with field for all samples when measured at the same temperature, irrespective of its absolute magnitude. As shown in Fig. S3 of the Supplemental Material [32], the (normalized) residual MR at $T = 15\text{K}$ is indeed found to follow the same form right across the phase diagram. Secondly, when the residual MR for one sample is plotted versus H/T for a range of temperatures inside the QC fan (see Fig. S4 of the Supplemental Material [32]), the data are found to collapse onto a single curve. Finally, as described in the Discussion section, a second sample with a doping close to x_c but with a larger residual resistivity (that effectively quenches the orbital component to the MR), is found to exhibit precisely the same MR scaling as seen in Ba122 and LCCO. Thus, we can conclude that the QC component to the MR in $\text{FeSe}_{1-x}\text{S}_x$ follows the exact same scaling relation, and since $d[\Delta\rho_{\text{QC}}]/dH = d[\delta\rho_{\text{QC}}]/dH$ (only the intercepts differ), we obtain from Eqs. (4) and (5) the following relation between β_{QC} and X_1 :

$$\beta_{\text{QC}} = \left(\frac{\sigma_{\text{QC}}}{\sigma_{\text{tot}}}\right)^2 X_1. \quad (6)$$

Thus, under the inference that the QC component to the MR in $\text{FeSe}_{1-x}\text{S}_x$ exhibits scale invariance, β_{QC} provides a direct measure of the contribution of σ_{QC} , the QC component, to the total conductivity. This quantity is plotted in Fig. 5 for

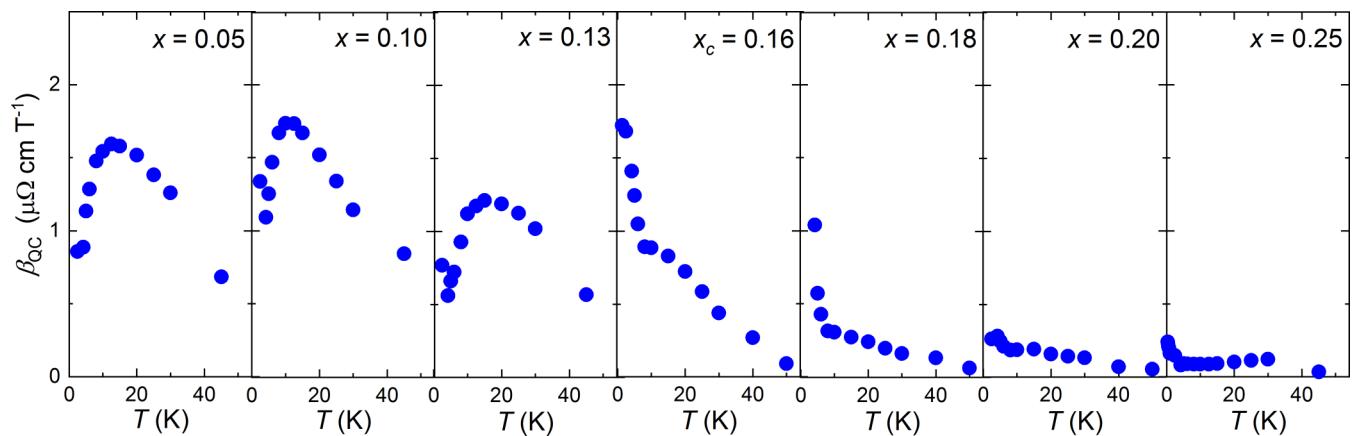


FIG. 5. Temperature and x dependence of β_{QC} , the strength of the H -linear transverse magnetoresistance in $\text{FeSe}_{1-x}\text{S}_x$ for all the Kyoto samples.

all the S concentrations studied (bar $x = 0.00$ for which β_{QC} is hard to extract due to its exceptional high-field behavior). What is most striking here is the evolution in the behavior of $\beta_{\text{QC}}[T]$ across the phase diagram. For samples with $x < x_c$, $\beta_{\text{QC}}[T]$ follows the same T dependence, reaching a maximum at or around the temperature below which $\rho(T)$ is no longer T linear, i.e., below the QC fan, implying that the QC component is reduced as one approaches the FL ($\rho \sim T^2$) regime (see Fig. 1) and may even vanish in the zero-temperature limit.

By contrast, for $x_c = 0.16$, β_{QC} increases monotonically with decreasing temperature, consistent with the observation that the T -linear resistivity extends down to the lowest T accessed to date and indicating that as the temperature is lowered, the QC component emerges as the dominant contribution. This nonmonotonic behavior of the H -linear component for $x < x_c$ and its correlation with the evolution of the zero-field resistivity is further evidence that it is not related to a contribution from Dirac-like states for which one would expect a monotonic increase in its magnitude as T decreases. Finally, beyond x_c , the magnitude of β_{QC} gradually softens with further S doping, though crucially, even for $x = 0.25$, β_{QC} remains finite.

Although β_{QC} is claimed to be proportional to $(\sigma_{\text{QC}}/\sigma_{\text{tot}})^2$, we cannot determine $\sigma_{\text{QC}}/\sigma_{\text{tot}}$ directly as we have no way of obtaining X_1 independently. However, one can gain an estimate for $\sigma_{\text{QC}}/\sigma_{\text{tot}}$ by simulating the zero-field $\rho(T)$ assuming parallel conduction, a point we shall return to later. Nevertheless, Fig. 5 reveals a very systematic evolution in the fraction of the total conductivity that can be attributed to the QC component.

For completeness, we now turn to consider the second component $\delta\rho_{\text{FL}} = \beta_{\text{FL}}(\mu_0 H)^2$. The large field range over which this MR component remains perfectly quadratic suggests that the electron and hole pockets in our $\text{FeSe}_{1-x}\text{S}_x$ crystals are close to being fully compensated. Moreover, as shown in Fig. 6(b) for the $x = 0.25$ sample, the T dependence of $\delta\rho_{\text{FL}}/\rho_{\text{FL}}[0]$ (where $\rho_{\text{FL}}[0] = \rho_{\text{FL}}[0, T]$ is estimated from the zero-field resistivity shown in Fig. 7 and discussed below) is found to have a Fermi-liquid (FL) form; $\delta\rho_{\text{FL}}/\rho_{\text{FL}}[0] = (\omega_c \tau)^2 = 1/(A + BT^2)^2$ between 1 and 30 K (since for a FL, $1/\tau \propto T^2$). At the QCP, the T dependence of $\delta\rho_{\text{FL}}/\rho_{\text{FL}}[0]$ cannot be captured by the same expression [Fig. 6(a)].

Nevertheless, the very strong T dependence observed in both cases supports the notion that this contribution is controlled by orbital effects (i.e., by $\omega_c \tau$).

D. Two-component conductivity

The presence of two distinct components in the transverse MR of $\text{FeSe}_{1-x}\text{S}_x$ implies that there must also be two contributions to the zero-field conductivity, i.e., $\sigma_{\text{tot}} = \sigma_{\text{FL}} + \sigma_{\text{QC}}$; the first term giving rise to the conventional, orbital MR and the second to the QC quadrature term. While the QC component σ_{QC} is linked directly to β_{QC} through Eqs. (4) and (5), it cannot be determined uniquely since X_1 itself is not known. We can, however, allow the magnitude of X_1 to vary (recall that X_1 will have a unique value for each sample but its magnitude is independent of T) and inspect the resultant T dependence of $\rho_{\text{QC}} = 1/\sigma_{\text{QC}}$ and $\rho_{\text{FL}} = 1/\sigma_{\text{FL}} = 1/(\sigma_{\text{tot}} - \sigma_{\text{QC}})$ where $\sigma_{\text{tot}} = 1/\rho[0, T]$, in order to see whether or not a self-consistent picture for both the zero-field resistivity and the transverse MR emerges from the data.

Examples of this procedure are shown in Figs. 7(a) and 7(b) for the $x_c = 0.16$ and $x = 0.25$ samples with $X_1 = 2.5$ and 1.7, respectively. Here, we have ensured that the two components add in parallel to give the total, as-measured resistivity. $\rho_{\text{QC}}(T)$ is found to be T linear in both cases, at least up to 25 K. For $x = 0.25$, $\rho_{\text{FL}}(T)$ retains its T^2 character up to 30 K, even though the raw resistivity curve is quadratic only up to 12 K. For $x_c = 0.16$, $\rho_{\text{FL}}(T)$ shows an approximately quadratic (FL-like) T dependence (indicated by a dotted line) only below 15 K. Above 15 K, the form of $\rho_{\text{FL}}(T)$ deviates from its low- T form and tends towards a constant value. The presence of the quasiparticle component in both the zero-field resistivity and the transverse MR may indicate that this sample is located close to, though not necessarily at the QCP. Further measurements down to lower temperatures (in higher fields) would be helpful in confirming the form of $\beta_{\text{QC}}/\beta_{\text{FL}}$ at $x = x_c$ below 1.5 K.

V. DISCUSSION

The observation of two distinct components in the transverse MR of $\text{FeSe}_{1-x}\text{S}_x$ raises the question why previous

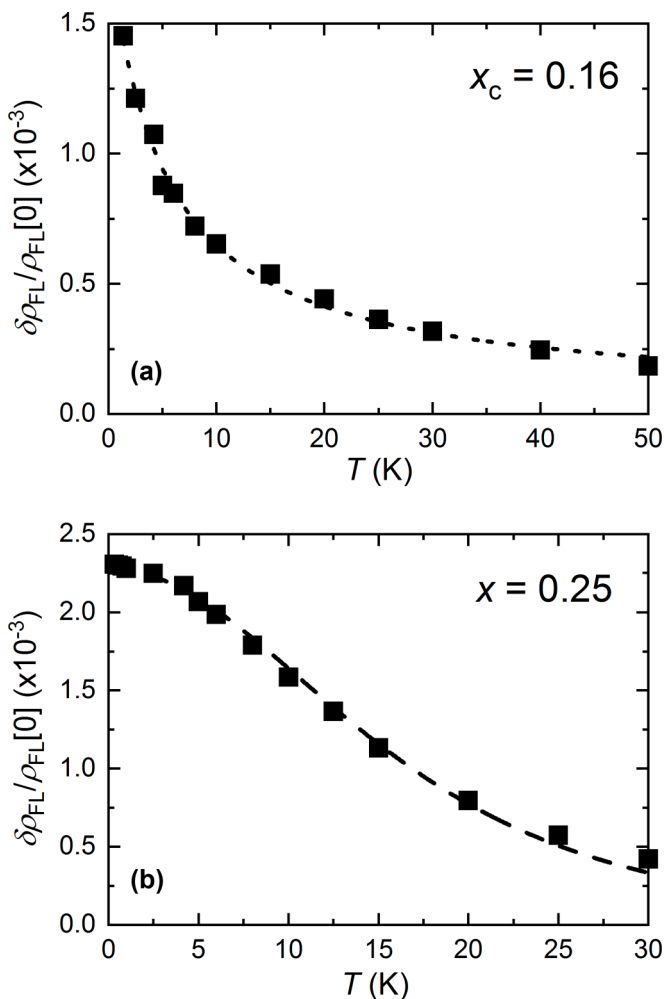


FIG. 6. T dependence of $\delta\rho_{FL}/\rho_{FL}[0]$ (at $\mu_0H = 1$ T) for (a) $x_c = 0.16$ and (b) $x = 0.25$. The dotted line in panel (a) is a guide to the eye. The dashed line in panel (b) denotes a fit to the data to the expression $\delta\rho_{FL}/\rho_{FL}[0] = 1/(A + BT^2)^2$ up to 30 K, as expected in a correlated Fermi liquid.

studies of correlated metals (both in the vicinity of or far from a QCP) found only an orbital MR response (that may or may not have violated Kohler’s rule) or the quadrature scaling form, but never the combination [11,12]. A comparative study of two crystals with different levels of disorder, presented below, provides one possible explanation for these distinct behaviors.

Figure 8(a) shows the low- T resistivity of the two crystals in question (both with nominal composition $x = 0.18$). The crystal with the lower residual resistivity (S018a) was synthesized in Kyoto using identical starting constituents and growth conditions as the other crystals described in the preceding section. As with the other crystals from this source, it exhibits both components in the transverse MR that evolve with temperature as summarized in Figs. 4 and 5. The second crystal (S018b) was prepared in Berkeley using a different technique and found to have a residual resistivity that is approximately five times higher. A series of MR curves obtained on this crystal over a wide temperature range [$1.5\text{ K} < T < 80\text{ K}$] is shown in Fig. 8(b)]. In contrast to the multiple crossing

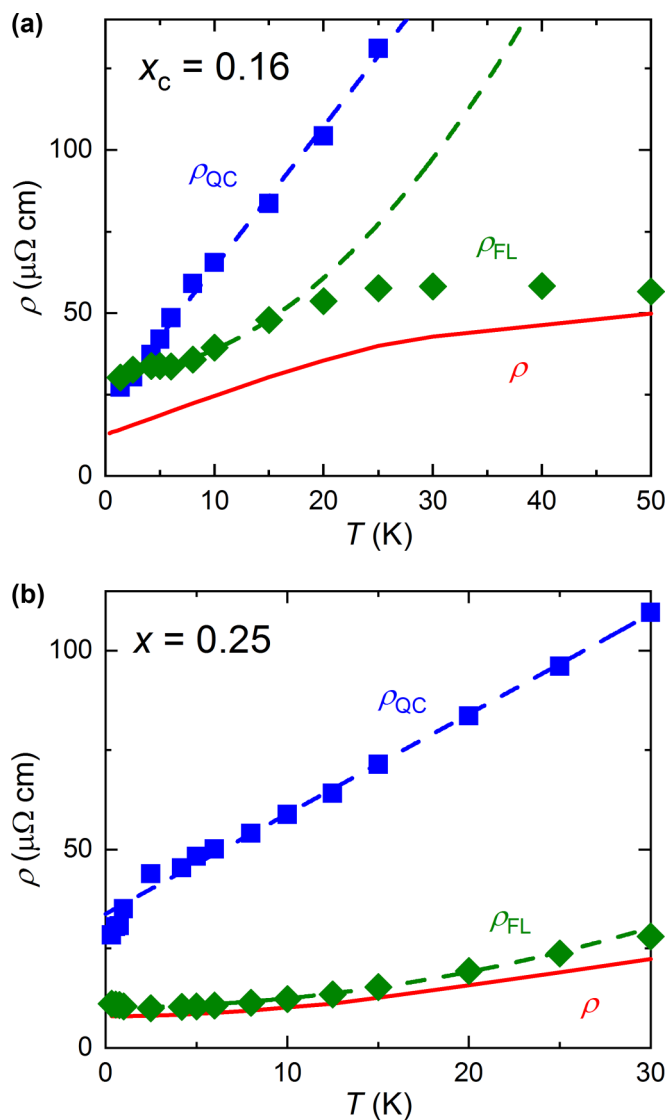


FIG. 7. Decomposition of experimentally determined $\rho(T)$ (solid lines) for (a) $\text{FeSe}_{0.84}\text{S}_{0.16}$ and (b) $\text{FeSe}_{0.75}\text{S}_{0.25}$ into quantum critical and quasiparticle channels obtained from the transverse MR study. The blue and green dashed lines represent T -linear and T^2 dependencies, respectively. In both cases, $1/\rho = 1/\rho_{FL} + 1/\rho_{QC}$.

points realized in the other crystals [an example of which is shown in Fig. 2(b)], the MR curves for S018b (beyond the field-induced superconductor-to-metal transition) are parallel to one another and become H linear at high fields. Moreover, when the MR curves are replotted as $\Delta\rho/T$ versus H/T , as shown in Fig. 8(c), they are found to collapse onto a single curve that fits the same quadrature form $\Delta\rho/T = \sqrt{1 + \gamma(\mu_B\mu_0H/k_B T)^2}$ (with $\gamma \approx 0.5$) that was observed in the cleaner crystal (though now unfettered by the presence of the orbital MR term).

The observation of QC scaling in the MR response of the second crystal reveals that while the orbital component is effectively quenched with increasing impurity scattering (a 5-fold increase in the residual resistivity would correspond to a 25-fold decrease in the orbital MR at low T), the QC component remarkably survives.

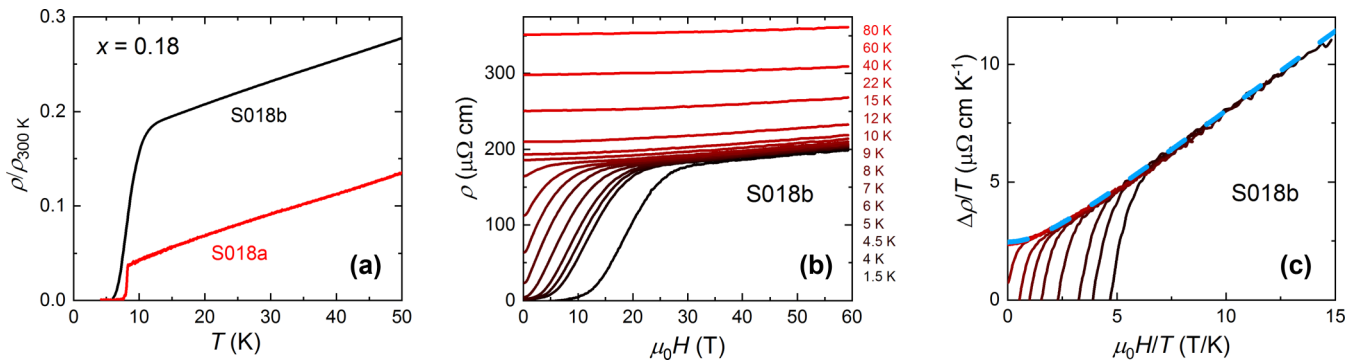


FIG. 8. (a) Zero-field resistivity for two $\text{FeSe}_{0.82}\text{S}_{0.18}$ crystals grown via different techniques (see text for details). (b) Set of transverse MR curves for S018b up to 60 T obtained at temperatures as labeled. (c) Scaling plot of $\Delta\rho/T$ vs μ_0H/T for S018b. The dashed line is the quadrature fit of the form $\sqrt{1 + \gamma(\mu_B\mu_0H/k_B T)^2}$ (with $\gamma \approx 0.5$).

It has been argued previously that the H -linear transverse MR and H/T scaling found in pnictides [6] and cuprates [8] may arise due to a variation in the carrier composition within a given sample [38], as postulated previously for two-dimensional electron gases [39] and even elemental metals [40]. The current study, however, suggests that this is not necessarily the case in QC systems. As shown in Fig. 4, the ratio of the H -linear (β_{QC}) to H^2 (β_{FL}) components shows a very systematic evolution with S substitution and peaks strongly at the QCP, even though the residual resistivities are comparable across the entire series of S-doped crystals [21]. Moreover, $\beta_{\text{QC}}/\beta_{\text{FL}}$ in FeSe is the same as in $\text{FeSe}_{0.75}\text{S}_{0.25}$, despite the fact that the former's residual resistivity is one order of magnitude smaller than the latter and clear quantum oscillations are observed in the former. Finally, the sharpness of the kinks in $d\rho/dT$ [21] at $T = T_s$ (for $x < x_c$) imply homogeneous doping for all these samples. Thus it appears unlikely that the H -linear component to the transverse MR is due to an extrinsic longitudinal contribution arising from a variation in carrier density along each crystal.

Recent models of strange metals, invoking either holographic methods [41] or based on the Sachdev-Ye-Kitaev picture of itinerant, nonquasiparticle transport [42], have succeeded in obtaining certain aspects of the MR scaling, but as of yet, not in tandem with a more conventional, orbital MR. The key task now therefore is to understand how these two components can coexist.

We consider here first the possibility that the two components arise from excitations that occupy different regions of the Brillouin zone. FeSe and its derivatives are known to contain (equal) numbers of electron- and holelike carriers and correlated metals often display an electron-hole dichotomy, most evident in the respective phase diagrams of electron- and hole-doped cuprates, for example [43]. In such a scenario, the electron and hole pockets found in $\text{FeSe}_{1-x}\text{S}_x$ would harbor different types of excitations that contribute respectively to the orbital and QC MR responses. Alternatively, the two excitations may reside within both pockets, albeit at different points on the Fermi surface; for example, the QC component may arise from excitations near hot spots—strong scattering sinks that destroy the quasiparticle character of excitations there—leading to strong momentum-dependent scattering as realized, for example, in the cuprates [44]. Indeed, the superconducting

gap in FeSe has been shown to be strongly anisotropic in both the electron and hole pockets, indicating anisotropic (and possibly orbitally selective) pairing interactions [45]. Both scenarios, however, appear inconsistent with the observation of quantum oscillations on both the electron and hole pockets (at least for S concentrations located away from the QCP) that indicate the presence of coherent quasiparticle states around the Fermi surface of both pockets [46,47].

The lack of oscillations at $x = x_c$ itself, however, is consistent with the notion that the quasiparticles are much heavier close to the QCP where the QC component of the MR is also dominant. The gradual crossover from quantum critical to quasiparticle contributions to the MR away from the QCP suggests in fact that the low-lying excitations near the Fermi level have dual character, i.e., the quasiparticle and the quantum critical sectors are two “flip sides” of the same electronic states, whose weighting depends on their proximity to the QCP. Whatever the origin, these findings clearly call for further theoretical studies in order to understand the interplay of the two sectors across the phase diagram, and more experimental studies to determine quantitatively the role of disorder in the realization of the H/T scaling in the transverse MR not only in more disordered $\text{FeSe}_{1-x}\text{S}_x$, but also in other candidate QC systems. The latter comparison is important to establish whether it is merely a question of disorder or length scales (e.g., between electron-electron collisions and electron-impurity collisions), or whether it is the nematic character of the quantum fluctuations in $\text{FeSe}_{1-x}\text{S}_x$ that allows both the quantum critical and quasiparticle sectors to reveal themselves, even at the QCP itself.

VI. CONCLUSIONS

In summary, we have carried out a systematic study of the transverse MR in a series of $\text{FeSe}_{1-x}\text{S}_x$ single crystals in high magnetic fields up to 38 T for S concentrations that span the nematic QCP. The field derivatives of the MR curves reveal the ubiquitous presence of two distinct (and additive) components to the MR in $\text{FeSe}_{1-x}\text{S}_x$: the normal orbital H^2 MR and an anomalous component that follows precisely the quadrature scaling first observed in the iron pnictide P-doped BaFe_2As_2 near the spin-density-wave QCP.

The ratio of the two MR components follows a very similar evolution with doping as the (renormalized) A coefficient of the T^2 resistivity, suggesting that the component with the quadrature form is associated with scale-invariant quantum critical fluctuations that are also responsible for the quasi-particle mass enhancement on approaching the QCP. The quantum critical contribution is found to become enhanced with decreasing T at the QCP, but is suppressed inside the FL regime away from the QCP. With increased disorder content, the orbital MR is quenched, leading to the appearance of strict quantum critical scaling at or near the QCP.

These collective findings provide evidence for the coexistence of two charge sectors in a quantum critical system whose relative weighting evolves systematically with proximity to the QCP. The task now is to identify how these two sectors coexist and to establish whether this is a universal behavior in quantum critical systems that, until now, may have been obscured by the presence of disorder.

ACKNOWLEDGMENTS

The authors would like to thank M. Bristow, A. Coldea, B. Goutraux, M. Katsnelson, A. Krikun, P. Reiss, K. Schalm,

and J. Schmalian for enlightening discussions on the work presented here. We also acknowledge the support of the HFML-RU/NWO, a member of the European Magnetic Field Laboratory (EMFL), and the NHMFL Pulsed Field Facility at Los Alamos, New Mexico. This work is part of the research programme Strange Metals (Grant No. 16METL01) of the former Foundation for Fundamental Research on Matter (FOM), which is financially supported by the Netherlands Organisation for Scientific Research (NWO). A portion of this work was also supported by the Engineering and Physical Sciences Research Council (Grant No. EP/L015544/1) and by Grants-in-Aid for Scientific Research (KAKENHI) (Grants No. JP15H02106, No. JP15H03688, No. JP15KK0160, No. JP18H01177, No. JP18H05227, and No. JP19H00649) and Innovative Areas Topological Material Science (Grant No. JP15H05852) and Quantum Liquid Crystals (Grant No. JP19H05824) from the Japan Society for the Promotion of Science (JSPS). V.N. and N.M. were supported by the Gordon and Betty Moore Foundations EPiQS Initiative through Grant No. GBMF4374. J.G.A. acknowledges partial support from the Center for Novel Pathways to Quantum Coherence in Materials, an Energy Frontier Research Center funded by the US Department of Energy, Office of Science, Basic Energy Sciences.

-
- [1] S. Sachdev, *Quantum Phase Transitions* (Cambridge University Press, Cambridge, UK, 2011).
- [2] H. V. Löhneysen, S. Mock, A. Neubert, T. Pietrus, A. Rosch, A. Schröder, O. Stockert, and U. Tutsch, *J. Magn. Magn. Mater.* **177-181**, 12 (1998).
- [3] J. Custers, P. Gegenwart, H. Wilhelm, K. Neumaier, Y. Tokiwa, O. Trovarelli, C. Geibel, F. Steglich, C. Pépin, and P. Coleman, *Nature (London)* **424**, 524 (2003).
- [4] J. A. N. Bruin, H. Sakai, R. S. Perry, and A. P. Mackenzie, *Science* **339**, 804 (2013).
- [5] H. V. Löhneysen, *J. Phys.: Condens. Matter* **8**, 9689 (1996).
- [6] I. M. Hayes, R. D. McDonald, N. P. Breznay, T. Helm, P. J. W. Moll, M. Wartenbe, A. Shekhter, and J. G. Analytis, *Nat. Phys.* **12**, 916 (2016).
- [7] I. M. Hayes, Z. Hao, N. Maksimovic, S. K. Lewin, M. K. Chan, R. D. McDonald, B. J. Ramshaw, J. E. Moore, and J. G. Analytis, *Phys. Rev. Lett.* **121**, 197002 (2018).
- [8] T. Sarkar, P. R. Mandal, N. R. Poniatowski, M. K. Chan, and R. L. Greene, *Sci. Adv.* **5**, eaav6753 (2019).
- [9] Recall that while $\Delta\rho$ is obtained by subtracting the effective zero-temperature, zero-field resistivity value of ρ , $\delta\rho$ is obtained by subtracting the 0 T resistivity value at the temperature of each field sweep.
- [10] A. B. Pippard, *Magnetoresistance in Metals* (Cambridge University Press, Cambridge, UK, 1989).
- [11] J. M. Harris, Y. F. Yan, P. Matl, N. P. Ong, P. W. Anderson, T. Kimura, and K. Kitazawa, *Phys. Rev. Lett.* **75**, 1391 (1995).
- [12] Y. Nakajima, H. Shishido, H. Nakai, T. Shibauchi, K. Behnia, K. Izawa, M. Hedo, Y. Uwatoko, T. Matsumoto, R. Settai, Y. Ōnuki, H. Kontani, and Y. Matsuda, *J. Phys. Soc. Jpn.* **76**, 024703 (2007).
- [13] P. Giraldo-Gallo, J. A. Galvis, Z. Stegen, K. A. Modic, F. F. Balakirev, J. S. Betts, X. Lian, C. Moir, S. C. Riggs, J. Wu, A. T. Bollinger, X. He, I. Božović, B. J. Ramshaw, R. D. McDonald, G. S. Boebinger, and A. Shekhter, *Science* **361**, 479 (2018).
- [14] K. K. Huynh, Y. Tanabe, and K. Tanigaki, *Phys. Rev. Lett.* **106**, 217004 (2011).
- [15] H.-H. Kuo, J.-H. Chu, S. C. Riggs, L. Yu, P. L. McMahon, K. De Greve, Y. Yamamoto, J. G. Analytis, and I. R. Fisher, *Phys. Rev. B* **84**, 054540 (2011).
- [16] S. Ishida, T. Liang, M. Nakajima, K. Kihou, C. H. Lee, A. Iyo, H. Eisaki, T. Kakeshita, T. Kida, M. Hagiwara, Y. Tomioka, T. Ito, and S. Uchida, *Phys. Rev. B* **84**, 184514 (2011).
- [17] S. Hosoi, K. Matsuura, K. Ishida, H. Wang, Y. Mizukami, T. Watashige, S. Kasahara, Y. Matsuda, and T. Shibauchi, *Proc. Natl. Acad. Sci. USA* **113**, 8139 (2016).
- [18] S.-H. Baek, D. V. Efremov, J. M. Ok, J. S. Kim, J. van den Brink, and B. Büchner, *Nat. Mater.* **14**, 210 (2015).
- [19] M. D. Watson, T. K. Kim, A. A. Haghighirad, N. R. Davies, A. McCollam, A. Narayanan, S. F. Blake, Y. L. Chen, S. Ghannadzadeh, A. J. Schofield, M. Hoesch, C. Meingast, T. Wolf, and A. I. Coldea, *Phys. Rev. B* **91**, 155106 (2015).
- [20] M. D. Watson, T. K. Kim, A. A. Haghighirad, S. F. Blake, N. R. Davies, M. Hoesch, T. Wolf, and A. I. Coldea, *Phys. Rev. B* **92**, 121108(R) (2015).
- [21] S. Licciardello, J. Buhot, J. Lu, J. Ayres, S. Kasahara, Y. Matsuda, T. Shibauchi, and N. E. Hussey, *Nature (London)* **567**, 213 (2019).
- [22] X. Wang and E. Berg, *Phys. Rev. B* **99**, 235136 (2019).
- [23] M. Bendele, A. Amato, K. Conder, M. Elender, H. Keller, H.-H. Klauss, H. Luetkens, E. Pomjakushina, A. Raselli, and R. Khasanov, *Phys. Rev. Lett.* **104**, 087003 (2010).
- [24] P. Wiecki, M. Nandi, A. E. Böhrer, S. L. Bud'ko, P. C. Canfield, and Y. Furukawa, *Phys. Rev. B* **96**, 180502(R) (2017).
- [25] V. Grinenko, R. Sarkar, P. Materne, S. Kamusella, A. Yamamshita, Y. Takano, Y. Sun, T. Tamegai, D. V. Efremov,

- S.-L. Drechsler, J.-C. Orain, T. Goko, R. Scheuermann, H. Luetkens, and H.-H. Klaus, *Phys. Rev. B* **97**, 201102(R) (2018).
- [26] K. Matsuura, Y. Mizukami, Y. Arai, Y. Sugimura, N. Maejima, A. Machida, T. Watanuki, T. Fukuda, T. Yajima, Z. Hiroi, K. Y. Yip, Y. C. Chan, Q. Niu, S. Hosoi, K. Ishida, K. Mukasa, S. Kasahara, J. G. Cheng, S. K. Goh, Y. Matsuda, Y. Uwatoko, and T. Shibauchi, *Nat. Commun.* **8**, 1143 (2017).
- [27] P. Wiecki, K. Rana, A. E. Böhmer, Y. Lee, S. L. Bud'ko, P. C. Canfield, and Y. Furukawa, *Phys. Rev. B* **98**, 020507(R) (2018).
- [28] M. W. Ma, D. N. Yuan, Y. Wu, X. L. Dong, and F. Zhou, *Physica C* **506**, 154 (2010).
- [29] Y. Sun, S. Pyon, and T. Tamegai, *Phys. Rev. B* **93**, 104502 (2016).
- [30] P. M. C. Rourke, A. F. Bangura, C. Proust, J. Levallois, N. Doiron-Leyraud, D. LeBoeuf, L. Taillefer, S. Adachi, M. L. Sutherland, and N. E. Hussey, *Phys. Rev. B* **82**, 020514(R) (2010).
- [31] J. S. Kim, *J. Appl. Phys.* **86**, 3187 (1999).
- [32] See Supplemental Material at <http://link.aps.org/supplemental/10.1103/PhysRevResearch.1.023011> for derivatives obtained from MR sweeps performed on the other S-doped single crystals, two-component analysis of the MR response of pristine FeSe, and tests of scale invariance in the residual transverse MR of FeSe_{1-x}S_x.
- [33] A. A. Abrikosov, *Phys. Rev. B* **58**, 2788 (1998).
- [34] K. K. Huynh, Y. Tanabe, T. Urata, H. Oguro, S. Heguri, K. Watanabe, and K. Tanigaki, *Phys. Rev. B* **90**, 144516 (2014).
- [35] S. Y. Tan, Y. Fang, D. H. Xie, W. Feng, C. H. P. Wen, Q. Song, Q. Y. Chen, W. Zhang, Y. Zhang, L. Z. Luo, B. P. Xie, X. C. Lai, and D. L. Feng, *Phys. Rev. B* **93**, 104513 (2016).
- [36] M. Čulo *et al.* (unpublished).
- [37] N. E. Hussey, A. P. Mackenzie, J. R. Cooper, Y. Maeno, S. Nishizaki, and T. Fujita, *Phys. Rev. B* **57**, 5505 (1998).
- [38] J. Singleton, [arXiv:1810.01998](https://arxiv.org/abs/1810.01998).
- [39] T. Khouri, U. Zeitler, C. Reichl, W. Wegscheider, N. E. Hussey, S. Wiedmann, and J. C. Maan, *Phys. Rev. Lett.* **117**, 256601 (2016).
- [40] G. J. C. L. Bruls, J. Bass, A. P. van Gelder, H. van Kempen, and P. Wyder, *Phys. Rev. Lett.* **46**, 553 (1981).
- [41] S. Cremonini, A. Hoover, and L. Li, *J. High Energy Phys.* **10** (2017) 133.
- [42] A. A. Patel, J. McGreevy, D. P. Arovas, and S. Sachdev, *Phys. Rev. X* **8**, 021049 (2018).
- [43] N. P. Armitage, P. Fournier, and R. L. Greene, *Rev. Mod. Phys.* **82**, 2421 (2010).
- [44] N. E. Hussey, J. Buhot, and S. Licciardello, *Rep. Prog. Phys.* **81**, 052501 (2018).
- [45] P. O. Sprau, A. Kostin, A. Kreisel, A. E. Böhmer, V. Taufour, P. C. Canfield, S. Mukherjee, P. J. Hirschfeld, B. M. Andersen, and J. C. Davis, *Science* **357**, 75 (2017).
- [46] T. Terashima, N. Kikugawa, A. Kiswandhi, E.-S. Choi, J. S. Brooks, S. Kasahara, T. Watashige, H. Ikeda, T. Shibauchi, Y. Matsuda, T. Wolf, A. E. Böhmer, F. Hardy, C. Meingast, H. V. Löhneysen, M. T. Suzuki, R. Arita, and S. Uji, *Phys. Rev. B* **90**, 144517 (2014).
- [47] A. I. Coldea, S. F. Blake, S. Kasahara, A. A. Haghighirad, M. D. Watson, W. Knafo, E.-S. Choi, A. McCollam, P. Reiss, T. Yamashita, M. Bruma, S. C. Speller, Y. Matsuda, T. Wolf, T. Shibauchi, and A. J. Schofield, *npj Quantum Mater.* **4**, 2 (2019)